

# Monte Carlo modeling of radiation dose distributions in intravascular radiation therapy

Michael G. Stabin<sup>a)</sup>

*Universidade Federal de Pernambuco, Recife, Brazil*

Mark Konijnenberg

*Mallickrodt, B.V., Petten, The Netherlands*

F. F. Knapp, Jr.

*Oak Ridge National Laboratory, Oak Ridge, Tennessee*

Robert H. Spencer

*University of Tennessee, Knoxville, Tennessee*

(Received 26 May 1999; accepted for publication 9 February 2000)

Radiation dose distributions are developed for balloon and wire sources of radioactivity within coronary arteries. The Monte Carlo codes MCNP 4B and EGS4 were used to calculate dose distributions for photons and electrons at discrete energies around such sources, with and without the presence of a high-density atherosclerotic plaque. An interactive computer program was developed which then calculates dose distributions for many radionuclides by applying the emission spectra to the discrete energy grids calculated by the Monte Carlo codes, weighting appropriately for electron energy and abundance. Results for Re-186 and Re-188 balloon sources are shown in comparison to an Ir-192 wire source. The program provides dose distributions as well as estimates of activity levels needed to deliver prescribed doses to the vessel wall at selected distances from the lumen in a selected time interval. In addition, dose calculations are presented in this paper for other organs in the body, from photon radiation as well as from possible loss of liquid activity into the bloodstream in the case of a balloon rupture. These results, especially the interactive computer program permitting easy comparison of various radionuclides and their physical characteristics, will greatly facilitate the comparison process and aid in the selection of the best candidate(s) for clinical use. © 2000 American Association of Physicists in Medicine. [S0094-2405(00)02005-8]

Key words: dosimetry, intravascular radiation therapy, radiation safety

## I. INTRODUCTION

The effectiveness of using high-dose-rate intravascular radioisotope sources for the inhibition of arterial restenosis has been demonstrated in a variety of animal models and clinical trials.<sup>1</sup> This new technology has been applied primarily to the coronary arteries for the inhibition of intimal hyperplasia. It is an abnormal hyperplastic response of the intima which causes restenosis following balloon angioplasty and/or stent placement. The current concept of the mechanism of action is based on the inhibition of myofibroblast stimulation in the adventitia by radiation.<sup>2</sup> In the postangioplasty patient, neointimal hyperplasia can be considered pathologic, as the narrowing or restenosis of a coronary artery can be life threatening.<sup>2,3</sup> Waksman and Wiedermann have demonstrated that vessel wall irradiation with beta particles prevents the onset of restenosis after stent implantation or angioplasty in a porcine model.<sup>4-7</sup> Calculation of the radiation dose delivered to the coronary artery wall, as well as to other organs and tissues in the body, is important to fully evaluate the possible risks and benefits of this promising new procedure. Computational methods for these calculations are well developed and simply need to be implemented appropriately. Both analytical and Monte Carlo methods are available; Monte Carlo methods have the advantage of explicit treat-

ment of the radiation transport of electrons and photons at interfaces of materials of different density and composition (e.g., at the interface of an atherosclerotic plaque and soft tissue). The different approaches to the delivery of this radiation dose include the use of radioactive wires or balloons filled with radioactive solutions. There are also numerous candidate radionuclides, including beta emitters and gamma emitters, low and high energy, which are currently under investigation. In this paper, radiation dose distributions around blood vessels of three diameters for balloon and wire sources are developed, using the Monte Carlo codes MCNP 4B and EGS4. A computer program, specifically developed to facilitate comparisons between different candidate radionuclides, source activities, and geometries is also described. In addition, doses to other organs of the patient, from the radioactive source, or from possible free radionuclide in the body, are given.

## II. METHODS

To calculate the electron and photon doses to the walls of the arteries in radiation transport simulations, both the MCNP 4B<sup>8</sup> and the EGS4<sup>9</sup> codes were employed. The vessel was modeled as a cylinder comprised of soft tissue and filled with water, with elemental composition and density values of

TABLE I. Elemental compositions and densities of the materials modeled (% by weight).

Element	Water	Soft tissue	Plaque	Wire
H	11.2	10.45	5.6	...
C	...	22.66	36.75	0.1
N	...	2.49	1.75	...
O	88.8	63.52	27.25	...
Na	...	0.112	...	...
Mg	...	0.013	...	...
Si	...	0.030	...	...
P	...	0.134	9.35	...
S	...	0.204	...	...
Cl	...	0.133	...	...
K	...	0.208	...	...
Ca	...	0.024	19.1	...
Cr	...	...	...	19.0
Fe	...	0.005	...	71.9
Ni	...	...	...	9.0
Zn	...	0.003	...	...
Rb	...	0.001	...	...
Zr	...	0.001	...	...
I	...	...	...	...
Density (g/cc):	1.00	1.04	2.02	7.80

these materials as shown in Table I.<sup>10</sup> To cover the size range of normal human coronary arteries, diameters of 1.5, 3, and 4.5 mm were selected for the calculations. The length of the cylinder was set at 30 mm, which was selected to be long relative to the path length of most beta particles. Thus, for the purpose of calculating the electron dose delivered to the wall, the geometry would appear to be that of an infinite cylinder for electron sources. For photons, we know that there will be some nonuniformity along the length, especially at the ends. Radiation doses were calculated at various distances into the artery wall by scoring the energy deposition in concentric cylinders of 10  $\mu\text{m}$  thickness around the artery.

One source geometry employed was a centrally positioned wire, with activity uniformly distributed throughout, whose elemental composition and density are also shown in Table I.<sup>11</sup> The other geometry was a balloon filled with radioactive solution. In the latter geometry, a central guide wire of 0.31 mm diameter was assumed, in a guide tube of 0.56 mm diameter, whose material characteristics were assumed to be similar to that of water. In this model the balloon filled the remainder of the vessel; for example, in the 4.5 mm diameter vessel, either to a radius of 2.25 mm (in the portion of the vessel without plaque) or 1.25 mm (in the portion with plaque). These dimensions were meant to be representative of some balloons in common use; specific geometries of individual balloons or devices may vary and may affect the dose calculations. The artery was assumed to have a deposition of plaque halfway around the artery wall. Plaque depositions are generally not distributed symmetrically throughout the vessel wall, being irregularly deposited over some or all of the wall. Although it is not possible to consider all plaque geometries in computer simulations; the geometry employed here has anticipated use in calculating

TABLE II. Geometries employed in the artery models.

	Vessel diameter		
	1.5 mm	3.0 mm	4.5 mm
Wire radius (mm)	0.15	0.15	0.15
Guide tube radius (mm)	0.28	0.28	0.57
Vessel radius to edge of plaque (mm)	0.50	1.00	1.25
Lumen radius (mm)	0.75	1.50	2.25

radiation doses (1) near such depositions and (2) in portions of the vessel wall that have little or no plaque buildup. Another complication is that plaques vary in density and average atomic number. When plaque is first laid down, it is relatively soft and may not be much different than soft tissue, for the purposes of radiation transport and attenuation. More mature plaque, however, incorporates much more calcium and can have a high density and average atomic number, including the presence of high-density fibrous tissue and hydroxyapatite.<sup>12,13</sup> The elemental composition and density assumed for the plaque studied here (Table I) was for a more mature plaque, and was chosen to have a relatively high  $Z$  and high density. The dimensions of the different structures in the three vessel geometries studied are shown in Table II. Example plots of the geometries are shown in Figs. 1 and 2.

Results were obtained from the Monte Carlo codes for electrons and photons at nine discrete energies. Sufficient particle histories were run to obtain relative errors of less than 5% in all cases, except for doses at long distances from low or moderate energy electron sources, where only bremsstrahlung radiation contributed to the dose, and errors could be substantial although contributions are minimal. Radiation doses were scored in concentric shells from 0.1 to 2.7 mm from the luminal surface of each vessel. The radiation dose delivered to the wall of the artery and surrounding tissues depends on the thickness of the artery wall, the presence of plaque, the source of radiation, and perhaps other considerations. The surrounding medium, whether artery wall or myocardial tissue, is well represented by the composition assumed for soft tissue (Table I). Results from the two codes were generally combined using a simple arithmetic average.

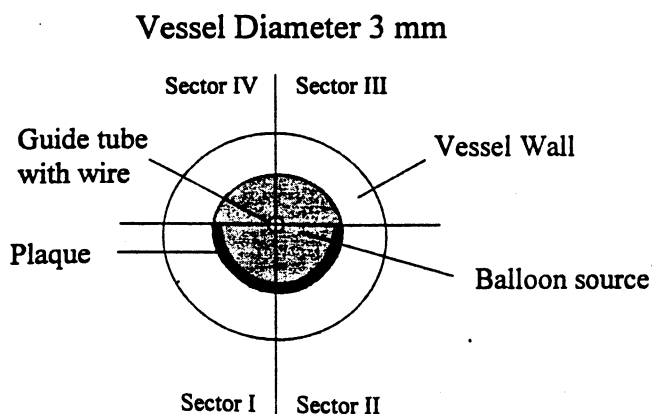


FIG. 1. Representation of a 3 mm diameter vessel with a balloon source.



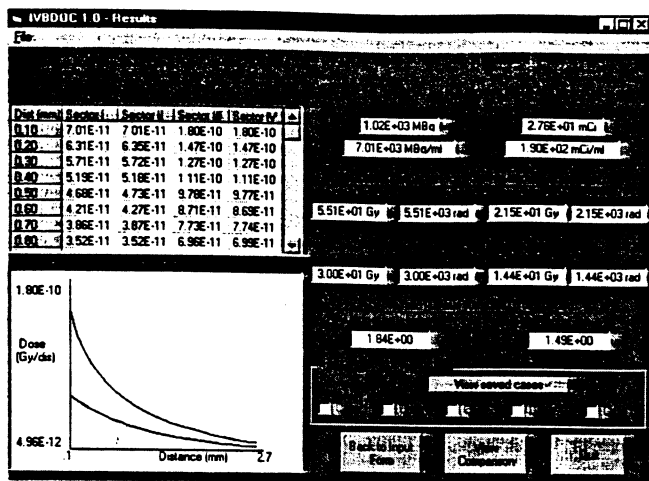


FIG. 4. First output screen from the interactive computer program: dose distributions and statistics regarding activity, dose ratios, etc.

depths in the vessel wall, for the user-selected dwell time and the value of activity needed to give the user-selected dose, are shown in the upper right box of the screen. Figure 6 shows the results of the comparison in further detail. A smaller intima to target dose ratio will allow the delivery of more radiation to the target tissue with a lower dose to the intimal surface of the vessel.

Radiation doses to other organs of the body from photon radiation are given in Table XV. Iridium-192 has the highest dose to adjacent tissues with the lungs, liver, adrenals, breasts, stomach, pancreas and thymus receiving from  $1.21 \times 10^{-3}$  to  $3.76 \times 10^{-3}$  Gy per GBq. With Re-186 or Re-188 the highest organ doses are about 10- to 100-fold less per GBq, demonstrating one benefit of using beta irradiation for this application. Since the computer program predicts about tenfold less activity is needed for a Re-186 or Re-188 balloon source than for an Ir-192 wire source, this suggests that

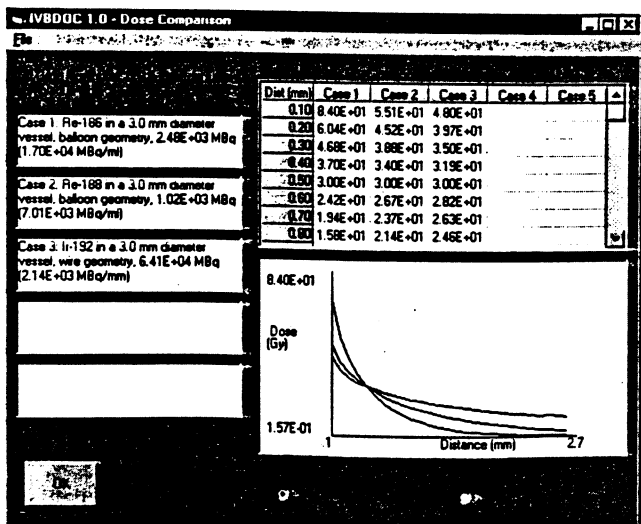


FIG. 5. Second output screen from the interactive computer program: comparison of doses from saved cases.

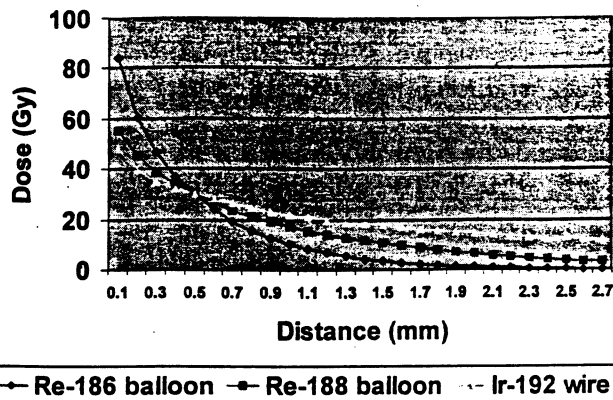


FIG. 6. Dose comparison for a Re-186 and Re-188 balloon and an Ir-192 wire in a 3 mm diameter vessel. In all cases, the activities were calculated so that the vessel would receive a dose of 30 Gy in 5 mins at 0.5 mm from the vessel surface (comparisons performed on the nonplaque side of the vessel). The calculated activities were Re-186, 2.48 GBq; Re-188, 1.02 GBq; and Ir-192, 64.1 GBq.

the organ doses realized in practice will then be perhaps 100- to 1000-fold lower for rhenium balloon sources than for Ir-192 wire sources.

Organ doses for the four radiopharmaceuticals assuming release of unit quantities into the bloodstream are shown in Table XVI. For P-32 and Y-90, the organ receiving the highest dose is red marrow with a dose of 8.12 and 3.26 Gy per GBq, respectively. With Re-186 and Re-188, the organs receiving the highest dose are the large intestine, thyroid, and urinary bladder.

#### IV. DISCUSSION

The results for electrons and photons from the two codes correlated well. There are some systematic differences at higher energies, particularly at very short ranges; details regarding these differences will be discussed in a separate paper. But these differences were relatively small, given the considerable uncertainties expected in clinical practice. Dose distributions for electrons drop more rapidly than for photons, until the range of the particle was reached, at which point only a bremsstrahlung contribution is seen. Doses on the plaque side of the vessel are considerably lower than on the nonplaque side, particularly for electrons. In some cases, low- to moderate-energy electrons do not penetrate the plaque to any significant degree. Electron doses from wire sources are somewhat lower than for balloon sources, as some attenuation occurred in the vessel surrounding the wire before the electrons reach the wall.

As noted in Sec. II, the artery was modeled as a cylinder of length 30 mm, and the doses in the concentric cylinders of tissue leading away from the vessel were averaged over this length. For electrons, this will give a reasonable approximation to the dose at most points along the source, but there will be some dose dropoff near the ends. As the artery will, of course, be longer than 30 mm, and the sources themselves may be longer and of variable length, the dose dropoff at the ends is difficult to predict. Thus, the doses calculated here

TABLE XV. Organ doses due to photon radiation from sources in the heart wall.

	Gy/GBq in the heart wall for 0.25 h			Gy/GBq in the heart wall per min		
	Ir-192	Re-186	Re-188	Ir-192	Re-186	Re-188
Adrenals	1.51E-03	4.32E-05	1.06E-04	1.01E-04	2.88E-06	7.07E-06
Brain	2.96E-05	2.99E-07	2.04E-06	1.97E-06	1.99E-08	1.36E-07
Breasts	1.52E-03	4.02E-05	1.07E-04	1.01E-04	2.68E-06	7.13E-06
Gallbladder wall	6.67E-04	1.73E-05	4.66E-05	4.45E-05	1.15E-06	3.11E-06
LLI wall	4.55E-05	6.24E-07	3.13E-06	3.03E-06	4.16E-08	2.09E-07
Small intestine	1.42E-04	2.55E-06	9.49E-06	9.47E-06	1.70E-07	6.33E-07
Stomach	1.33E-03	4.09E-05	9.83E-05	8.87E-05	2.73E-06	6.55E-06
ULI wall	1.74E-04	3.46E-06	1.16E-05	1.16E-05	2.31E-07	7.73E-07
Kidneys	4.35E-04	1.11E-05	3.13E-05	2.90E-05	7.40E-07	2.09E-06
Liver	1.21E-03	3.59E-05	8.76E-05	8.07E-05	2.39E-06	5.84E-06
Lungs	2.26E-03	7.18E-05	1.64E-04	1.51E-04	4.79E-06	1.09E-05
Muscle	5.02E-04	1.43E-05	3.59E-05	3.35E-05	9.53E-07	2.39E-06
Ovaries	6.02E-05	7.31E-07	3.91E-06	4.01E-06	4.87E-08	2.61E-07
Pancreas	1.79E-03	5.53E-05	1.31E-04	1.19E-04	3.69E-06	8.73E-06
Red marrow	6.41E-04	1.59E-05	4.39E-05	4.27E-05	1.06E-06	2.93E-06
Bone surfaces	5.14E-04	2.81E-05	4.58E-05	3.43E-05	1.87E-06	3.05E-06
Skin	2.29E-04	5.37E-06	1.60E-05	1.53E-05	3.58E-07	1.07E-06
Spleen	8.36E-04	2.52E-05	6.21E-05	5.57E-05	1.68E-06	4.14E-06
Testes	9.35E-06	7.05E-08	6.94E-07	6.23E-07	4.70E-09	4.63E-08
Thymus	3.76E-03	1.18E-04	2.75E-04	2.51E-04	7.87E-06	1.83E-05
Thyroid	2.58E-04	5.58E-06	1.80E-05	1.72E-05	3.72E-07	1.20E-06
Urinary bladder wall	1.76E-05	2.60E-07	1.30E-06	1.17E-06	1.73E-08	8.67E-08
Uterus	5.63E-05	6.50E-07	3.66E-06	3.75E-06	4.33E-08	2.44E-07

TABLE XVI. Organ doses from injection of radionuclides into the bloodstream due to balloon rupture (Gy per GBq injected).<sup>a</sup>

	P-32	Y-90	Re-186	Re-188
Adrenals	7.60E-01	9.07E-02	3.17E-02	4.45E-02
Brain	7.60E-01	9.07E-02	3.10E-02	4.35E-02
Breasts	7.60E-01	9.07E-02	3.09E-02	4.34E-02
Gallbladder wall	7.60E-01	9.07E-02	3.38E-02	4.66E-02
LLI wall	7.60E-01	9.07E-02	1.95E+00	1.97E+00
Small intestine	7.60E-01	9.07E-02	3.66E-02	4.97E-02
Stomach	7.60E-01	9.07E-02	2.64E-01	4.33E-01
ULI wall	7.60E-01	9.07E-02	1.95E+00	1.98E+00
Heart wall	7.60E-01	9.07E-02	3.14E-02	4.42E-02
Kidneys	7.60E-01	9.07E-02	3.20E-02	4.48E-02
Liver	7.60E-01	3.89E+00	3.18E-02	4.46E-02
Lungs	7.60E-01	9.07E-02	3.13E-02	4.38E-02
Muscle	7.60E-01	9.07E-02	3.18E-02	4.45E-02
Ovaries	7.60E-01	9.07E-02	3.67E-02	4.99E-02
Pancreas	7.60E-01	9.07E-02	3.24E-02	4.55E-02
Red marrow	8.12E+00	3.26E+00	3.19E-02	4.48E-02
Bone surfaces	1.04E+01	3.91E+00	3.32E-02	4.52E-02
Skin	7.60E-01	9.07E-02	3.10E-02	4.35E-02
Spleen	7.60E-01	9.07E-02	3.19E-02	4.48E-02
Testes	7.60E-01	9.07E-02	3.18E-02	4.47E-02
Thymus	7.60E-01	9.07E-02	3.12E-02	4.38E-02
Thyroid	7.60E-01	9.07E-02	6.06E-01	1.10E+00
Urinary bladder wall	1.91E+00	8.02E-01	1.04E+00	1.51E+00
Uterus	7.60E-01	9.07E-02	3.52E-02	4.87E-02
Total body	1.52E+00	5.21E-01	4.37E-02	5.74E-02

<sup>a</sup>Chemical forms assumed: P-32 as sodium phosphate, Y-90 in ionic form, and Re-186 and Re-188 as perrhenate.

have some uncertainties due to this averaging, but, in our experience with photon emitters such as Ir-192, this overall effect should be of the order of 5% (although some doses very near the ends, over short distances, may be different than the average by larger amounts).

It is important to note that explicit consideration of balloon wall thickness was not included in the code (thus the diameters stated for the balloons are inner, not outer, diameters). Balloon walls vary between manufacturers, but are generally of the order of 0.05 mm. As the composition of the balloon wall is not much different from that of soft tissue, consideration of different balloon wall thicknesses may be made by evaluating the doses reported by the program at the distance reported adjusted for the assumed balloon wall thickness (e.g., if the program reports the dose at 0.5 mm and the balloon wall thickness is 0.05 mm, this would occur at a distance of 0.45 mm from the balloon wall surface).

The computer program, designed in Microsoft Visual Basic (© Microsoft Corporation, 1997), gives radiation dose distributions for most emitters within 1–5 s on a Pentium-II personal computer (this program may be downloaded currently from the ftp site <ftp.orau.gov>; specific instructions may be obtained from the first author). The program is quite easy to understand and use. Figure 3 shows the input screen, where a user can select the radionuclide and geometry, and specify the dose desired, the time in which the dose is to be delivered, and the distance into the vessel wall that the dose will be delivered. Figure 4 shows the first output screen, which gives the dose distribution radially into the vessel wall, and some statistics about the amount of activity needed to give the dose specified by the user, the dose at the luminal surface and the dose at the depth specified on the first screen as well as the ratio of these doses. The user then has the option of saving this as a case, and returning to the first screen to select more radionuclides and/or geometries. Figure 5 shows the comparison screen, in which doses from between two to five nuclides and/or geometries can be compared, using a commonly selected dose/time/distance combination. The comparison is initially made on the side of the vessel that does not contain the atherosclerotic plaque, but an option is included to provide the comparison on the side that does contain plaque. Most information from the output screens can be printed or saved to a file. Figure 6 shows a comparison between Re-186 and Re-188 balloon sources and an Ir-192 wire source in a 3 mm diameter vessel. In all cases, the activities were calculated so that the vessel would receive a dose of 30 Gy in 5 min at 0.5 mm from the vessel surface (comparisons performed on the nonplaque side of the vessel). The calculated activities were Re-186, 2.48 GBq; Re-188, 1.02 GBq; and Ir-192, 64.1 GBq.

Our experience with the calculations led us to choose the nine discrete energies to cover the range of energies likely to be encountered. The spacing between energy values was chosen based on this experience to limit the spread of the results and make the interpolation process sound. A logarithmic interpolation was chosen to further limit the possibility of inaccuracies in the interpolation process, and we believe that the results reported are sound. Furthermore, we per-

formed separate calculations with the Monte Carlo codes for a number of radionuclides using their explicit decay spectrum, and compared them with the interpolated results. Differences were minor in all cases, of the order of 5%, well within the range of other potential errors and uncertainties likely to be encountered in application of these values.

There are certain inescapable limitations of the modeling process in approximating physical realities. In clinical situations, physicians may encounter many different artery geometries, plaque deposition configurations, plaque compositions, etc. All of these considerations cannot be well considered in a code such as this one which provides rapid comparisons of dose distributions in arteries with and without plaque for a large number of radionuclides in a few artery sizes and source configurations [the program at present treats only wire or liquid-filled (not gas-filled) balloons, and cannot consider every possible source configuration]. The geometry of the balloon source here may not represent well the exact geometry encountered, but the dose distributions on either side of the artery are reasonable, given the complete absence of plaque or the presence of a relatively high-density plaque. Care must be taken in interpreting these results in comparison to real clinical situations, as with any model-based simulation.

Table XV shows the radiation doses to other organs, which are not very high compared to the doses received by the structures immediately around the vessel, but should be included in an overall evaluation of the risks of the procedure. Due to the high-photon component, and the higher amounts of activity needed, Ir-192 will give a considerably higher dose to other organs of the body (not to mention the attending medical staff, whose analysis was deemed outside the scope of this paper) than a pure beta emitter or a nuclide with a lower abundance of photons relative to electrons, such as Re-188.

According to the program, one would require 1.04 GBq of P-32 or 0.92 GBq of Y-90 in a balloon source to give the dose noted above (30 Gy in 5 min at 0.5 mm in a 3 mm diameter artery). It is clear from these data and the dose estimates in Table XVI that, in the case of a balloon rupture, use of P-32 or Y-90 in the forms assumed here (liquid sources of P-32 as phosphate or ionic Y-90) will represent a significant risk to the patient, as the predicted absorbed doses to red marrow from the quantities of activity assumed are near or above median lethal doses. For the rhenium isotopes, there are significant doses predicted to the intestines, but not at levels that would be considered life threatening. Other strategies may improve the radiation dose picture, such as the use of perchlorate to block thyroid uptake, or attaching the rhenium isotopes to other chemical compounds, such as MAG3, and obtain different biological behavior.

The probability of a balloon rupture is small, as inflation pressures used for intravascular radiation therapy are lower than those used in the practice of angioplasty. Nonetheless, given the large number of procedures expected to be performed each year, it seems likely that eventually an incident will occur, and a judicious choice must be made of the radionuclides to be employed (indeed other incidents, such as

embolization of sources due to broken catheters or wires, are possible and have occurred, and we do not treat every potential risk of these procedures here). Naturally, many other factors are involved as well, including clinical efficacy, risks of radiation dose to other organs of the patient and the medical staff (especially in the case of photon emitters), logistic criteria, half-life of the radionuclide, disposal methods, credentialing and licensure, and other factors. Accurate knowledge of the radiation dose distributions is an important key to this choice. The results presented here, especially the interactive computer program permitting easy comparison of various radionuclides and their physical characteristics, should greatly facilitate the comparison process and aid in the selection of the best candidate(s) for clinical use, for the cases considered.

<sup>3</sup>Electronic mail: stabin@npd.ufpe.br

<sup>1</sup>R. Waksman, *Vascular Brachytherapy*, 2nd ed. (Futura, Armonk, NY, 1999).

<sup>2</sup>J. Wilcox, R. Waksman, S. King, and N. Scott, "The role of the adventitia in the arterial response to angioplasty: the effect of intravascular radiation." *Int. J. Radiat. Oncol., Biol., Phys.* **36**, 789–796 (1996).

<sup>3</sup>Y. Shi, M. Pieniek, A. Fard, J. O'Brien, J. D. Mannion, and A. Zaleski, "Adventitial remodeling after coronary arterial injury," *Circulation* **93**, 340–348 (1996).

<sup>4</sup>R. Waksman, K. A. Robinson, I. R. Crocker, M. B. Gravanis, S. J. Palmer, C. Wang, G. D. Cipolla, and S. B. King III, "Intracoronary radiation before stent implantation inhibits neointima formation in stented porcine coronary arteries," *Circulation* **92**, 1383–1386 (1995).

<sup>5</sup>R. Waksman, K. A. Robinson, I. R. Crocker, C. Wang, M. B. Gravanis, G. D. Cipolla, R. A. Hillstead, and S. B. King III, "Intracoronary low-dose beta-irradiation inhibits neointima formation after coronary artery balloon injury in the swine restenosis model," *Circulation* **92**, 3025–3031 (1995).

<sup>6</sup>R. Waksman, K. A. Robinson, I. R. Crocker, M. B. Gravanis, G. D. Cipolla, and S. B. King III, "Endovascular low-dose irradiation inhibits neointima formation after coronary artery balloon injury in swine," *Circulation* **91**, 1533–1539 (1995).

<sup>7</sup>J. Wiedermann, C. Marboe, H. Amols, A. Schwartz, and J. Weinberger, "Intracoronary irradiation markedly reduces restenosis after balloon angioplasty in a porcine model," *J. Am. Coll. Cardiol.* **23**, 1491–1498 (1994).

<sup>8</sup>J. Briesmeister, "MCNP—A general Monte Carlo  $n$ -particle transport code," MCNP User's Manual, Los Alamos National Laboratory, 1993.

<sup>9</sup>A. Bielajew and D. Rogers, "PRESTA: the parameter reduced electron-step transport algorithm for electron monte carlo transport," *Nucl. Instrum. Methods. B* **18**, 165–181 (1987).

<sup>10</sup>M. Cristy and K. Eckerman, "Specific absorbed fractions of energy at various ages from internal photons sources," ORNL/TM-8381 V1-V7, Oak Ridge National Laboratory, Oak Ridge, TN, 1987.

<sup>11</sup>CRC Press, *The CRC Handbook of Chemistry and Physics*, 57th ed., edited by R. Weast (CRC, Cleveland, OH, 1976).

<sup>12</sup>S. Mautner, F. Lin, G. Mautner, and W. Roberts, "Comparison in women versus men of composition of atherosclerotic plaques in native coronary arteries and in saphenous veins used as aortocoronary conduits," *J. Am. Coll. Cardiol.* **21**, 1312–1318 (1994).

<sup>13</sup>L. Fitzpatrick, A. Severson, W. Edwards, and R. Ingram, "Diffuse calcification in human coronary arteries. Association of osteopontin with atherosclerosis," *J. Clin. Invest.* **94**, 1597–1604 (1994).

<sup>14</sup>International Commission on Radiological Protection, *Radionuclide Transformations—Energy and Intensity of Emissions*, ICRP Publication 38 (Pergamon, Oxford, 1983).

<sup>15</sup>D. Weber, K. Eckerman, L. Dillman, J. Ryman, *MIRD: Radionuclide Data and Decay Schemes* (Society of Nuclear Medicine, New York, 1989).

<sup>16</sup>F. Fritsch and R. Carlson, "Monotone Piecewise Cubic Interpolation," *SIAM (Soc. Ind. Appl. Math.) J. Numer. Anal.* **17**, 238–246 (1980).

<sup>17</sup>M. Stabin, "MIRDOSE—the personal computer software for use in internal dose assessment in nuclear medicine," *J. Nucl. Med.* **37**, 538–546 (1996).

<sup>18</sup>International Commission on Radiological Protection, *Limits for Intakes of Radionuclides by Workers*, ICRP Publication 30 (Pergamon, New York, 1979).

<sup>19</sup>K. Lathrop, H. Atkins, M. Berman, M. Hays, and E. Smith, "MIRD Dose Estimate Report No. 8—Summary of Current Radiation Dose Estimates to Normal Humans from  $^{99m}\text{Tc}$  as Sodium Pertechnetate," *J. Nucl. Med.* **17**, 74–77 (1976).

<sup>20</sup>J. Kotzerke, S. Fenchel, A. Guhlmann, M. Stabin, M. Rentschler, F. Knapp, Jr., and S. Reske, "Pharmacokinetics of  $^{99m}\text{Tc}$ -pertechnetate and  $^{188}\text{Re}$ -perrhenate after oral administration of perchlorate: Option for subsequent care after the use of liquid  $^{188}\text{Re}$  in a balloon catheter," *Nucl. Med. Comm.* **19**, 795–801 (1998).

<sup>21</sup>See EPAPS Document No. E-PAPSE-MPHYA6-27-020005 for 12 tables on recommended doses per disintegration. This document may be retrieved via the EPAPS homepage (<http://www.aip.org/pubservs/epaps.html>) or from <ftp.aip.org> in the directory /epaps/. See the EPAPS homepage for more information.